



U-series zircon age constraints on the plumbing system and magma residence times of the Changbai volcano, China/North Korea border

Haibo Zou ^{a,*}, Qicheng Fan ^b, Hongfu Zhang ^c, Axel K. Schmitt ^d

^a Department of Geology and Geography, Auburn University, Auburn, AL 36849, USA

^b Institute of Geology, China Earthquake Administration, Beijing 100029, China

^c Institute of Geology and Geophysics, Chinese Academy of Sciences, Beijing 100029, China

^d Department of Earth and Space Sciences, UCLA, Los Angeles, CA 90095, USA



ARTICLE INFO

Article history:

Received 17 February 2014

Accepted 28 April 2014

Available online 9 May 2014

Keywords:

Changbai volcano

Young zircons

U-series disequilibrium

Magma plumbing system

Magma residence times

ABSTRACT

The Changbai (or Baitoushan, Paektu) volcano on the China/North Korea border is best known for its climactic caldera-forming eruption of 100 km^3 of comendite materials 1000 years (1 ka) ago. The polygenetic Changbai volcano also erupted moderate-volume pre-caldera comendite lava at ~4 ka and small-volume post-caldera trachyte ignimbrite at ~0.3 ka. Here we report ^{238}U - ^{230}Th disequilibrium ages of zircons from lavas and ignimbrites of the pre-caldera (~4 ka), syn-caldera (1 ka), and post-caldera (~0.3 ka) events. The zircon isochron ages are $12.2 \pm 1.1 \text{ ka}$ (2σ) for the 4-ka comendite lava and $12.2 \pm 1.7 \text{ ka}$ for the 1-ka comendite ignimbrite. Zircons from the 0.3-ka trachyte ignimbrite exhibit 3 respective peaks at $2.6 \pm 1.8 \text{ ka}$, $130 \pm 10 \text{ ka}$ and $>230 \text{ ka}$. The indistinguishable zircon ages for the 4-ka pre-caldera eruption of comendite lava and the 1-ka caldera-forming eruption of comendite pumice and ignimbrite suggest that the 4-ka lava provides an early sampling of a much larger magma body at depth and thus serves as a kind of petrologic early-warning signal. In addition, the 4-ka lava may represent the lowest-temperature magma in the roof zone of a thermally zoned magma chamber that usually escapes first. The distinctive multi-modal zircon age distributions of the 0.3-ka trachytic eruption, however, reveal that this post-caldera eruption tapped a different magma body and indicate that Changbai's magmatic plumbing system had changed after the 1-ka caldera-forming climactic eruption. Our results suggest very short zircon and magma residence times for the Changbai volcano (8 kyr for the 4-ka eruption, 11–12 kyr for the 1-ka eruption and 2.3 kyr for the 0.3-ka eruption).

© 2014 Elsevier B.V. All rights reserved.

1. Introduction

Recently, the Changbai (or Baitoushan, Paektu) volcano located at the border of China and North Korea has drawn much attention as a result of its large climactic Millennium Eruption (Stone, 2011, 2013) and due to the recent detection of swarms of small tremors at the volcano between 2002 and 2006 (Wei et al., 2013; Xu et al., 2012). The Changbai volcano erupted approximately 100 km^3 of comendite materials about 1000 years ago (1 ka), and the collapse of the upper cone into the emptied magma chamber during this caldera-forming eruption produced a 5 km wide caldera (Dunlap et al., 1992; Liu et al., 1998; Machida and Arai, 1983; Wei et al., 2003). ^{14}C ages of charred wood buried by the eruption range from 935 AD to 1215 AD (Dunlap et al., 1992; Horn and Schmincke, 2000; Liu et al., 1998; Wei et al., 2007). More recent and thorough ^{14}C age studies indicate a smaller eruption age range between 935 and 946 AD (Nakamura et al., 2007; Xu et al., 2012). This so-called Millennium Eruption is one of the two largest eruptions that

occurred on Earth in the past 2000 years, rivaling the 1815 Tambora eruption (Self et al., 1984) in Indonesia. The Millennium Eruption mainly produced rhyolitic pumice, ash, and ignimbrite. The fallout fan from the Plinian and co-ignimbrite ash extends as far as north Japan, ~1200 km (Fig. 1).

In addition to the 1-ka Millennium Eruption, the Changbai volcano erupted moderate-volume pre-caldera comendite lava at ~4 ka (Liu et al., 1998; Yin et al., 1999) and small-volume post-caldera trachyte ignimbrite at ~0.3 ka (Ji et al., 1999; Liu et al., 1998). Earlier magmatic stages at the Changbai volcano include a shield-forming (Miocene to 1 Ma) basaltic lava plateau that covers an area of 7200 km^2 centered at the Changbai volcano, and the subsequent (1 Ma to 0.02 Ma) volcanic cone dominated by trachyte lavas (Liu et al., 1998).

In spite of recent extensive studies on the Changbai volcano, many important questions remain unresolved, including the evolution of the underlying plumbing system, the pre-eruption history, how the magmas may be related genetically, and finally the potential for future volcanic activity at Changbai. For example, it is unclear whether or not the pre-caldera 4-ka eruption of comendite lava shared the same magma chamber as the caldera-forming 1-ka explosive eruption and therefore served as a precursor for the major 1-ka eruption. It is also

* Corresponding author.

E-mail address: Haibo.zou@gmail.com (H. Zou).

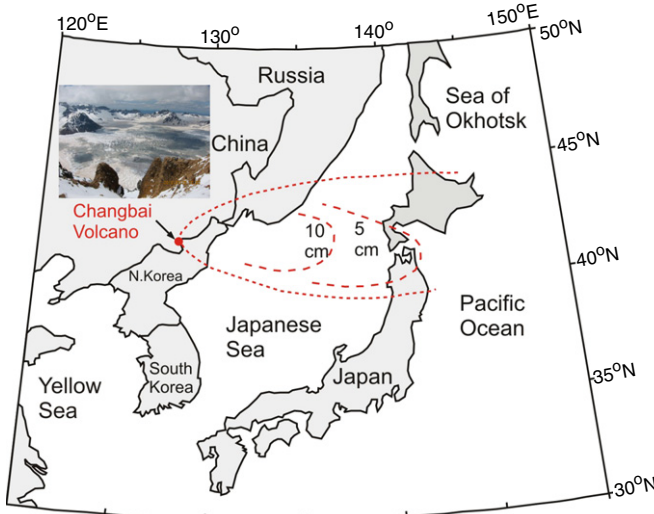


Fig. 1. Changbai volcano at the border between China and North Korea, and the distribution of tephras from the Changbai volcano. The isopach dashed lines represent distribution of comendite ash deposits from the 1-ka Millennium Eruption. Thickness values (in cm) are after Machida and Arai (1983). The inserted field photo is the caldera with a frozen Heavenly Lake (Tianchi).

not clear if the magma plumbing system changed after the 1-ka climactic eruption.

The eruption products of the Millennium Eruption, as well as the pre-caldera eruption and post-caldera eruption, contain valuable information concerning the magma plumbing system evolution and pre-eruption magma residence times. We collected samples of the 4-ka comendite lava from Qixiangzhan (QXZ) on the north flank, 1-ka comenditic ignimbrite from north caldera rim near Baiyanfeng, and 0.3-ka trachytic ignimbrite from Nanpo (south caldera rim) and Baguamiao (Fig. 2), and identified zircon crystals from all 3 eruption products. Recent development and refinement of high-spatial resolution ^{238}U - ^{230}Th disequilibrium geochronology has provided unique age determinations on young (<350 ka) zircons (Reid et al., 1997; Schmitt et al., 2010; Storm et al., 2011; Zou et al., 2010a). We dated the zircon crystals from these pre-caldera (4 ka), syn-caldera (1 ka) and post-caldera (0.3 ka) products using an ion microprobe CAMECA IMS 1270 at UCLA. The goals of this study are (1) to investigate if the magmas from these recent eruptions are genetically related and thus to reveal the evolution of the underlying volcanic system by comparing zircon age populations of all three eruptions and (2) to estimate crystal and magma residence times prior to each eruption.

2. Geological background and mineralogy of recent eruption products

The Changbai volcano is an intraplate stratovolcano located at the northeastern margin of the North China Craton. Its volcano cone sits on a 2–5 Ma trachybasalt shield (the Gaima plateau) that is underlain by Archean-Proterozoic metamorphic rocks of the North China Craton. The volcano lies roughly 1200 km west of the active Pacific subduction trench. It is the most active and largest volcano with felsic magma eruptions in northeast China. Previous studies have attributed the Changbai intraplate volcanism to (1) asthenosphere upwelling (Tatsumi et al., 1990) caused by the subduction of the Pacific plate or the Kula-Pacific ridge (Basu et al., 1991), the thickening of the stagnant Pacific slab (Zou et al., 2008), or by big mantle wedge processes in the upper mantle and mantle transition zone (Zhao et al., 2009), and to (2) continental rifting associated with development of the Japan Sea (Liu et al., 2001). It is reasonable to presume that the continental rifting may be related

to the deep asthenosphere upwelling in the region. Kuritani et al. (2009) proposed that the rate of asthenosphere upwelling in NE China has decreased with time since at least 4.2 Ma.

The most recent eruption products of the Changbai volcano include the 4-ka comendite lava, 1-ka comendite ignimbrite and pumice, and 0.3-ka trachytic ignimbrite. All of these eruption products contain sanidine, iron-rich clinopyroxene (e.g., hedenbergite), and iron-rich olivine (e.g., fayalite) crystals. Mineral chemical compositions for most eruption products have been documented earlier (Fan et al., 1999; Li et al., 2004; Liu et al., 2007; Zou et al., 2010a, 2010b) and are summarized here.

The 4-ka comendite lavas have a porphyritic texture. Phenocrysts consist primarily of sanidine (composition $\text{An}_{0-1}\text{Ab}_{58-61}\text{Or}_{39-41}$) and clinopyroxene (hedenbergite, $\text{Wo}_{45-46}\text{En}_{2-4}\text{Fs}_{50-51}$), with minor fayalite ($\text{Fo}_{0.5-1.8}$). The groundmass contains glass and microlites of sodic amphibole (ferro-richterite) and ilmenite (Fan et al., 1999; Liu et al., 2007).

The 1-ka comenditic ignimbrites are vesicular (10–20%) and are composed of glass and crystals of sanidine, and hedenbergite, with minor fayalite. New chemical analyses of the glass and minerals in these ignimbrites will be reported in Section 4.3. The 1-ka comenditic pumices are highly vesicular (70%) and are composed of glass and phenocrysts of sanidine ($\text{An}_{0-1}\text{Ab}_{62-63}\text{Or}_{36-37}$) (Zou et al., 2010b), hedenbergite ($\text{Wo}_{41-43}\text{En}_{0-4}\text{Fs}_{53-55}$), and minor fayalite ($\text{Fo}_{0.5-2.5}$) crystals (Fan et al., 1999).

The 0.3-ka trachytic ignimbrites are vesicular (10–20%) and contain sanidine ($\text{An}_{4.8}\text{Ab}_{49.7}\text{Or}_{45.5}$) (Fan et al., 1999), clinopyroxene ($\text{Wo}_{44.8}\text{En}_{13.2}\text{Fs}_{42}$) and minor olivine ($\text{Fo}_{10.3}$) crystals (Li et al., 2004).

3. Analytical methods

Several 0.4 cm diameter holes drilled into 1-inch (2.54 cm) diameter aluminum disks were filled with soft indium metal. Zircon grains were then pressed into the indium-filled disks to be dated by the U-series disequilibrium method.

Zircons were dated using shallow depth profiling (surface profiling) of unpolished zircons from all 4 samples (QXZ, BYFX, NP, BGM) and by conventional U-Th dating of polished zircon interiors from only 1 sample (BYFX). Zircon grains in the mount for surface profiling were oriented so that the zircon surface was at the same horizontal plane as the surface of the ion probe indium mount. The mount was subsequently cleaned, dried, and coated with gold without any polishing. Detailed analytical methods using ^{238}U - ^{230}Th surface profiling have been documented in Zou et al. (2010a) and Schmitt (2011). In comparison, zircon grains in separate mounts for conventional ^{238}U - ^{230}Th spot analyses were polished to section the crystals in half, then cleaned, dried, and coated with gold.

^{238}U - ^{230}Th disequilibrium dating was performed on individual zircon crystals using the UCLA CAMECA IMS 1270 secondary ion mass spectrometer (ion microprobe). A 35 to 45 nA mass-filtered $^{16}\text{O}^-$ beam was focused into a ~25 μm diameter oval spot. Secondary ions were accelerated at 10 keV with an energy bandpass of 50 eV and analyzed at a mass resolution of 5000. Intensities of $^{230}\text{Th}^{16}\text{O}^+$, $^{232}\text{Th}^{16}\text{O}^+$, and $^{238}\text{U}^{16}\text{O}^+$ were measured in each cycle. Reference species $^{90}\text{Zr}^{16}\text{O}_4$ was also measured. Background was measured at mass 246.3. Relative sensitivities for ^{238}UO and ^{232}ThO (and ^{230}ThO) were calibrated by measuring the radiogenic $^{206}\text{Pb}/^{208}\text{Pb}$ ratio of old, concordant reference zircons AS-3 from the Duluth Complex and 91,500 (Paces and Miller, 1993; Wiedenbeck et al., 1995). Each analysis run included 45 cycles with a typical duration time of about 25 min. Ion microprobe ($^{230}\text{Th}/^{232}\text{Th}$) and ($^{238}\text{U}/^{232}\text{Th}$) analyses with the CAMECA IMS 1270 routinely achieve a relative precision and accuracy of ~1–2% with a spot size of ~25 μm diameter and a depth resolution of <3 μm in single electron multiplier collector peak-jumping mode. Absolute ages can be calculated by isochron regression if the spread in U/Th is sufficiently large and mean square weighted deviation (MSWD) is small (<2.5) (Lowenstern et al.,

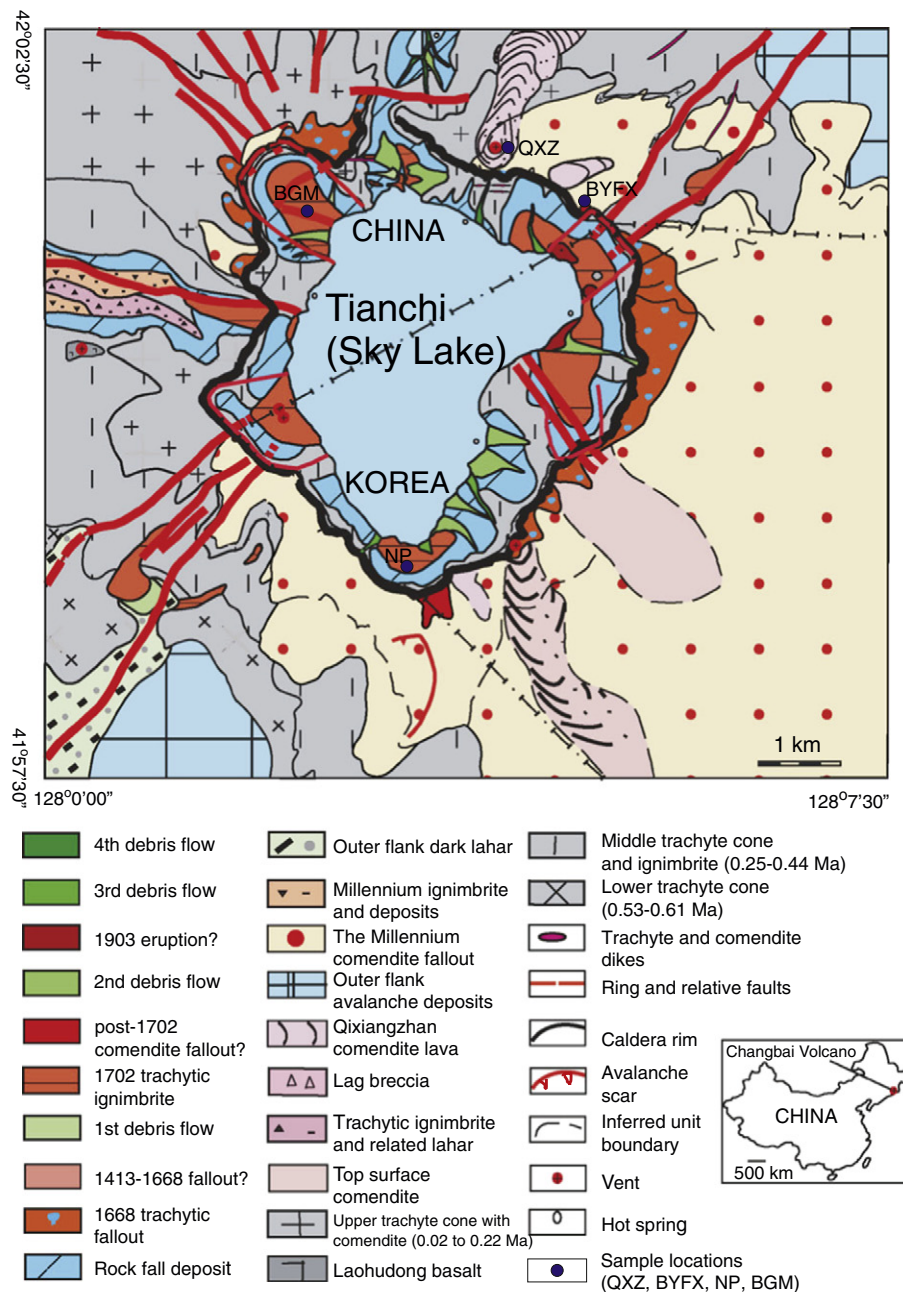


Fig. 2. Geological map of the Changbai volcanic cone and the Tanchi caldera lake.
Modified after Wei et al. (2013) and Wei et al. (2007).

2000). Alternatively, if the data points are scattered, then two-point isochron model ages can be calculated from SIMS zircon spot analyses and bulk glass (or whole-rock) isotope compositions with age uncertainties for individual zircons (Reid et al., 1997).

Whole-rock major element concentrations were measured by XRF at the Institute of Geology and Geophysics, Chinese Academy of Sciences, and at the GeoAnalytical Lab, Washington State University. Analytical methods and standards have been documented in Johnson et al. (1999) and Zhang et al. (2002).

Chemical compositions of alkali feldspar, clinopyroxene, fayalite, and glass from the 1-ka ignimbrite were analyzed by a JEOL JXA-8100 electron probe in the State Key Laboratory of Lithospheric Evolution, Institute of Geology and Geophysics, Chinese Academy of Sciences. Analytical methods for major elements have been documented in the

literature (e.g., Su et al., 2009; Zhao et al., 2009). Analytical conditions consisted of a 15 kV accelerating voltage and a 10 nA beam current. Beam diameters were 10 μm for glass analysis and 5 to 8 μm for feldspar analysis.

4. Results

4.1. Major elements

SiO_2 contents are 73.6 wt.% for the 4-ka lava, 72.6% for the 1-ka ignimbrite, and 64–66% for the two post-caldera 0.3-ka ignimbrites (Table 1). ##The 4-ka sample from Qixiangzhan (QXZ) and the 1-ka sample plot in the rhyolite field and the two 0.3-ka sample plots in the trachyte field in the TAS diagram (Fig. 3). All samples have high

Table 1

Major element compositions of whole-rock samples.

Samples	Eruption ages	SiO ₂	TiO ₂	Al ₂ O ₃	FeO	MnO	MgO	CaO	Na ₂ O	K ₂ O	P ₂ O ₅	LOI	TOTAL
QXZ	4 ka	73.64	0.25	11.53	3.88	0.07	0.16	0.21	4.6	4.61	0.00	0.32	99.27
BYFX	1 ka	72.62	0.23	10.93	4.09	0.08	0.00	0.30	5.52	4.54	0.01	0.62	98.95
NP	0.3 ka	66.26	0.39	14.68	4.79	0.13	0.09	1.09	5.57	5.42	0.05	0.72	99.35
BGM	0.3 ka	64.84	0.42	16.10	4.10	0.11	0.23	1.30	5.49	5.93	0.01	0.48	99.01

K₂O (4.5%–5.9%) and Na₂O (4.6%–5.6%). The 4-ka sample is a comendite lava and the 1-ka sample is a comenditic ignimbrite, while the 0.3-ka samples from Baguamiao and Nanpo are trachytic ignimbrites.

4.2. Zircon U-series ages

A total of 53 zircons from the 4-ka comendite lavas at QXZ were analyzed by surface profiling (Table 2), yielding a ²³⁸U–²³⁰Th isochron age of 12.2 ± 1.1 ka (2σ , MSWD = 0.73) (Fig. 4). Their U-Th isotope data, as well as two-point model ages given by referencing each zircon analysis to the whole rock, are presented in Table 2. The model age spectrum for the 4-ka eruption is unimodal. Individual zircon model ages range from 7 ka to 19 ka (Table 2).

Fifteen zircon grains from a 1-ka comendite ignimbrite sample (BYFX) were analyzed by surface profiling, forming an isochron age of 12.2 ± 1.7 ka (MSWD = 1.01) (Fig. 5). The model age spectrum for this 1 ka sample is also unimodal. Individual zircon model ages range from 8 ka to 18 ka. This isochron age from the 1-ka ignimbrite is consistent with a zircon isochron age of 10.6 ± 1.6 ka from a 1-ka comendite pumice sample (Zou et al., 2010b). Note that the zircon ages from the Millennium Eruption (both ignimbrite and pumice) and the 4-ka eruption are essentially identical and they all display unimodal age distributions.

Fourteen polished zircon interiors in a separate mount from the same 1-ka ignimbrite sample BYFX were analyzed by conventional spot analysis, forming an isochron age of 13.1 ± 1.8 ka (MSWD = 0.90) (Fig. 6). Individual zircon interior model ages vary from 9.9 ka to 20 ka. The zircon interior isochron age is 0.9 ka (=13.1–12.2 ka) older than the surface isochron age. But the uncertainty in the zircon

interior-rim age difference is 2.5 ka, according to error propagation (e.g., Zou, 2007, 2014). Therefore, there is no clearly resolvable difference (0.9 ± 2.5 ka) between the interior isochron age and surface isochron age for zircons from the 1-ka ignimbrite. The nearly identical rim and interior ages of the Changbai zircons are in contrast with the 40-kyr age span between zircon rim and interior from the Tengchong volcanics of the SE Tibetan Plateau (Tucker et al., 2013; Zou et al., 2010a).

Samples of the 0.3-ka trachytic eruption were collected from Nanpo (south caldera rim) and Baguamiao. A total of 25 zircons from the 0.3-ka eruption were analyzed by surface profiling, 9 from Nanpo, and 16 from Baguamiao. Their multi-modal zircon age populations are more complex than the uniform zircon ages for the 4-ka and 1-ka comenditic eruptions. Note that zircon model-age distributions for the 0.3-ka sample from Nanpo and Baguamiao are essentially identical (Fig. 7) and both have 3 peaks. When all zircons from the 0.3-ka eruption are combined together, zircon ages for the post-caldera 0.3-ka trachytic eruption define multimodal age populations with 3 peaks (Fig. 8). The youngest peak for the 0.3-ka eruption is 2.6 ± 1.8 ka ($n = 11$, MSWD = 0.90), an older peak is 130 ± 10 ka ($n = 13$, MSWD = 1.7), and the oldest population is >230 ka (near the ²³⁸U–²³⁰Th equilibrium).

The 12 ka zircons from the pre-caldera 4-ka comendite lavas and the 1-ka comenditic ignimbrite, as well as the 2.6 ka zircons from the 0.3-ka trachytic ignimbrite, represent some of the youngest zircons that have been dated by the U-series isochron method. Previously Condomines (1997) reported 12 ± 1 ka zircons in a trachyte from the Puy de Dôme (French Massif Central) using the U-series isochron method.

4.3. Mineral and glass compositions for 1-ka ignimbrite

Chemical compositions of alkali feldspar, clinopyroxene, fayalite, and glass from the 1-ka ignimbrite (measured by electron probe) are presented in Table 3. Average alkali feldspar composition is $\text{Or}_{35.8}\text{Ab}_{63.4}\text{An}_{0.8}$, and the alkali feldspar is sanidine with a low An number (<1%). Average clinopyroxene composition is $\text{Wo}_{45.1}\text{En}_{44.3}\text{Fs}_{50.6}$ and the clinopyroxene is hedenbergite. Average olivine composition is Fo_{2} . Glass compositions are enriched in SiO₂ (75%), Na₂O (5.5%) and K₂O (4.4%).

Note that the chemical compositions of sanidine, clinopyroxene, and fayalite from the 1-ka ignimbrite are essentially identical to the respective minerals from the 4-ka pre-caldera lava and the 1-ka pumice, but are different from the respective minerals from the 0.3-ka post-caldera trachytic ignimbrites that are more enriched in Ca and Mg.

5. Discussion

5.1. The 4 ka pre-caldera comendite lava as a precursor for the Millennium Eruption

The 4 ka comendite lava at QXZ contains zircons that are indistinguishable in U-series ages from those of the subsequent 1-ka caldera-forming Millennium Eruption of pumice and ignimbrite. Our U-series zircon data provide geochronological evidence that the pre-caldera 4-ka QXZ lava and the 1-ka Millennium Eruption sample shared the same magma chamber. This conclusion is also consistent with their similar Nd isotopic compositions. $^{143}\text{Nd}/^{144}\text{Nd}$ values are 0.512553 for the 4-ka

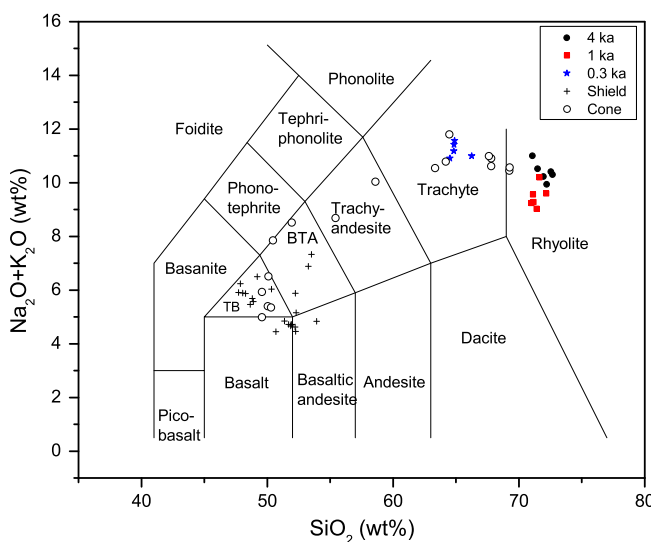


Fig. 3. Total alkali versus silica (TAS) plot.
Data sources: Fan et al. (2006), Liu et al. (1998) and this paper.

Table 2

U-Th isotopes, concentrations and model ages for zircons from 4 ka, 1 ka, and 0.3 ka eruptions.

(^{238}U / ^{232}Th)	1se	(^{230}Th / ^{232}Th)	1se	Th age	1s+	1s-	U	Th	m slope	Error slope
				ka	ka	ka	ppm	ppm		
<i>4 ka eruption (surface profiling)</i>										
zircon_QXZ@1	4.737	0.022	1.130	0.104	11.8	3.1	-3.0	290	186	0.10
zircon_QXZ@2	4.665	0.023	1.094	0.115	10.9	3.5	-3.4	254	165	0.10
zircon_QXZ@3	4.691	0.027	1.105	0.116	11.2	3.5	-3.4	272	176	0.10
zircon_QXZ@4	4.685	0.023	1.163	0.090	12.9	2.8	-2.7	235	152	0.11
zircon_QXZ@5	4.590	0.034	1.051	0.095	9.8	2.9	-2.8	223	148	0.09
zircon_QXZ@6	4.365	0.021	1.062	0.093	10.8	3.1	-3.0	305	212	0.09
zircon_QXZ@7	4.524	0.044	1.220	0.108	15.3	3.5	-3.4	237	159	0.13
zircon_QXZ@8	3.731	0.024	1.023	0.072	11.6	2.9	-2.8	321	261	0.10
zircon_QXZ@9	4.829	0.023	1.049	0.114	9.2	3.3	-3.2	201	126	0.08
zircon_QXZ@10	4.607	0.025	1.031	0.103	9.2	3.1	-3.0	233	154	0.08
zircon_QXZ@11	4.795	0.029	1.217	0.098	14.2	3.0	-2.9	255	161	0.12
zircon_QXZ@12	4.740	0.023	1.092	0.097	10.6	2.9	-2.8	258	165	0.09
zircon_QXZ@13	4.622	0.022	1.038	0.101	9.3	3.1	-3.0	257	169	0.08
zircon_QXZ@14	4.766	0.022	1.089	0.104	10.5	3.1	-3.0	276	176	0.09
zircon_QXZ@15	4.446	0.022	1.171	0.084	14.0	2.8	-2.7	261	178	0.12
zircon_QXZ@16	4.582	0.021	0.976	0.100	7.6	3.0	-2.9	308	204	0.07
zircon_QXZ@17	4.492	0.023	1.197	0.096	14.7	3.2	-3.1	303	205	0.13
zircon_QXZ@18	4.535	0.022	1.041	0.100	9.7	3.1	-3.0	360	241	0.08
zircon_QXZ@19	4.734	0.023	0.959	0.096	6.8	2.8	-2.7	322	207	0.06
zircon_QXZ@20	4.553	0.021	1.212	0.131	14.9	4.3	-4.1	243	162	0.13
zircon_QXZ@21	4.561	0.022	1.159	0.108	13.2	3.5	-3.3	290	193	0.11
zircon_QXZ@22	4.593	0.026	1.123	0.125	12.0	3.9	-3.8	197	130	0.10
zircon_QXZ@23	4.579	0.022	1.057	0.092	10.0	2.8	-2.8	256	170	0.09
zircon_QXZ@24	4.766	0.024	1.058	0.104	9.6	3.0	-3.0	250	159	0.08
zircon_QXZ@25	4.671	0.022	1.234	0.123	15.1	3.9	-3.7	241	157	0.13
zircon_QXZ@26	4.798	0.023	1.239	0.119	14.8	3.6	-3.5	262	166	0.13
zircon_QXZ@27	4.754	0.025	1.256	0.118	15.5	3.7	-3.6	267	170	0.13
zircon_QXZ@28	4.495	0.022	1.176	0.178	14.0	5.9	-5.6	423	286	0.12
zircon_QXZ@29	4.723	0.023	1.125	0.111	11.6	3.4	-3.3	258	166	0.10
zircon_QXZ@30	4.610	0.030	1.350	0.180	19.2	6.0	-5.7	273	180	0.16
zircon_QXZ@31	4.455	0.027	1.188	0.149	14.6	5.0	-4.8	256	175	0.12
zircon_QXZ@32	4.754	0.029	1.199	0.132	13.8	4.0	-3.9	284	181	0.12
zircon_QXZ@33	5.861	0.030	1.312	0.113	13.3	2.7	-2.6	279	144	0.11
zircon_QXZ@34	4.668	0.023	1.310	0.128	17.5	4.1	-4.0	280	182	0.15
zircon_QXZ@35	4.798	0.025	1.190	0.104	13.3	3.1	-3.1	247	156	0.12
zircon_QXZ@36	4.636	0.024	0.956	0.090	6.9	2.6	-2.6	248	163	0.06
zircon_QXZ@37	4.368	0.061	1.130	0.097	13.0	3.3	-3.2	264	184	0.11
zircon_QXZ@38	3.999	0.024	1.142	0.083	15.0	3.1	-3.0	283	215	0.13
zircon_QXZ@39	4.654	0.028	1.122	0.124	11.8	3.8	-3.7	193	126	0.10
zircon_QXZ@40	3.899	0.018	1.007	0.073	10.4	2.7	-2.7	319	248	0.09
zircon_QXZ@41	2.671	0.012	0.973	0.044	15.1	2.8	-2.7	504	573	0.13
zircon_QXZ@42	4.541	0.021	1.141	0.103	12.7	3.3	-3.2	219	146	0.11
zircon_QXZ@43	4.553	0.026	1.270	0.098	16.8	3.2	-3.1	205	137	0.14
zircon_QXZ@44	3.342	0.037	1.051	0.070	14.7	3.3	-3.2	350	317	0.13
zircon_QXZ@45	2.470	0.011	0.984	0.046	17.6	3.3	-3.2	538	661	0.15
zircon_QXZ@46	2.430	0.020	0.987	0.058	18.2	4.3	-4.2	323	403	0.15
zircon_QXZ@47	3.158	0.015	1.079	0.088	17.2	4.6	-4.4	443	425	0.15
zircon_QXZ@48	4.556	0.021	1.118	0.130	12.0	4.1	-4.0	303	202	0.10
zircon_QXZ@49	3.855	0.023	1.074	0.079	13.0	3.1	-3.0	394	310	0.11
zircon_QXZ@50	4.437	0.023	1.146	0.100	13.3	3.3	-3.2	247	169	0.11
zircon_QXZ@51	4.455	0.021	1.206	0.108	15.2	3.6	-3.5	234	159	0.13
zircon_QXZ@52	3.757	0.018	1.008	0.094	10.9	3.7	-3.6	247	199	0.10
zircon_QXZ@53	3.766	0.021	1.059	0.075	12.8	3.0	-2.9	367	296	0.11
Whole rock	0.634	0.010	0.711	0.010						0.02
<i>1 ka eruption (surface profiling)</i>										
BYFX@1	4.728	0.023	1.069	0.100	10.0	3.0	-2.9	261	167	0.09
BYFX@2	4.380	0.021	1.166	0.092	14.1	3.1	-3.0	237	164	0.12
BYFX@3	4.391	0.026	0.986	0.078	8.3	2.5	-2.4	296	204	0.07
BYFX@4	4.435	0.023	1.162	0.081	13.8	2.7	-2.6	272	186	0.12
BYFX@5	4.561	0.022	1.124	0.089	12.1	2.8	-2.8	272	181	0.11
BYFX@6	4.316	0.022	1.037	0.088	10.1	2.9	-2.8	389	273	0.09
BYFX@7	2.884	0.023	1.031	0.064	16.7	3.7	-3.6	577	607	0.14
BYFX@8	4.270	0.028	0.987	0.082	8.6	2.7	-2.6	292	208	0.08
BYFX@9	4.484	0.023	1.255	0.089	16.6	3.0	-2.9	259	175	0.14
BYFX@10	4.023	0.025	1.092	0.075	13.0	2.8	-2.7	402	303	0.11
BYFX@11	3.311	0.026	0.965	0.056	10.9	2.6	-2.5	393	360	0.09
BYFX@12	4.466	0.029	1.296	0.100	18.1	3.4	-3.3	241	163	0.15
BYFX@13	4.302	0.043	1.046	0.088	10.5	2.9	-2.8	563	397	0.09
BYFX@14	4.495	0.022	1.156	0.107	13.4	3.5	-3.4	273	184	0.12
BYFX@15	4.386	0.020	1.109	0.106	12.2	3.5	-3.4	321	222	0.11
WR rhyolite	0.634	0.012	0.711	0.014						0.03

(continued on next page)

Table 2 (continued)

	$(^{238}\text{U})/^{232}\text{Th}$	1se	$(^{230}\text{Th})/^{232}\text{Th}$	1se	Th age	1s +	1s -	U	Th	m	slope
					ka	ka	ka	ppm	ppm	slope	
<i>1 ka eruption (polished interior analysis)</i>											
BYFX@16	4.644	0.100	1.383	0.138	20.04	4.6	-4	178	104	0.17	0.03
BYFX@17	4.361	0.107	1.305	0.107	18.95	3.8	-4	338	236	0.16	0.03
BYFX@18	4.239	0.091	1.126	0.099	13.34	3.5	-3	222	142	0.12	0.03
BYFX@19	4.638	0.090	1.337	0.118	18.57	3.9	-4	233	137	0.16	0.03
BYFX@20	4.083	0.075	1.095	0.079	12.88	2.9	-3	223	166	0.11	0.02
BYFX@21	4.315	0.078	1.058	0.104	10.83	3.5	-3	192	135	0.09	0.03
BYFX@22	4.636	0.086	1.209	0.131	14.52	4.2	-4	155	101	0.12	0.03
BYFX@23	4.179	0.082	1.113	0.091	13.13	3.2	-3	199	145	0.11	0.03
BYFX@24	4.391	0.081	1.037	0.090	9.897	2.9	-3	225	155	0.09	0.02
BYFX@25	4.092	0.074	1.097	0.080	12.94	2.9	-3	223	165	0.11	0.02
BYFX@26	4.030	0.075	1.015	0.088	10.24	3.2	-3	234	176	0.09	0.03
BYFX@27	4.492	0.087	1.219	0.136	15.41	4.5	-4	180	122	0.13	0.04
BYFX@28	4.484	0.082	1.051	0.075	10.09	2.4	-2	245	166	0.09	0.02
BYFX@29	3.654	0.078	1.060	0.071	13.41	3	-3	270	225	0.12	0.02
WR rhyolite	0.634	0.012	0.711	0.014							
<i>0.3 ka eruption (surface profiling)</i>											
02NP3@1	4.519	0.103	0.760	0.080	1.4	2.3	-2.3	394	264	0.01	0.02
02NP3@2	3.765	0.086	2.950	0.231	137	34	-26	145	117	0.72	0.08
02NP3@3	5.221	0.057	3.411	0.334	97	21	-18	119	69	0.59	0.07
02NP3@4	4.726	0.108	0.824	0.088	3.1	2.5	-2.4	273	175	0.03	0.02
02NP3@5	4.309	0.121	0.691	0.126	0.0	-3.7	3.8	310	218	0.00	0.03
02NP3@6	3.363	0.045	2.671	0.175	139	29	-23	158	143	0.72	0.06
02NP3@7	4.403	0.110	0.890	0.159	5.3	5.0	-4.7	327	225	0.05	0.04
02NP3@8	4.188	0.105	0.917	0.128	6.5	4.2	-4.1	268	194	0.06	0.04
02NP3@9	3.657	0.093	3.397	0.290	239	243	-70	144	119	0.89	0.10
BGM@1	4.896	0.023	0.644	0.099	0.0	-2.5	2.5	230	142	0.00	0.02
BGM@2	4.913	0.027	0.805	0.104	2.6	2.7	-2.7	197	121	0.02	0.02
BGM@3	4.806	0.030	0.698	0.112	0.0	-2.9	3.0	207	131	0.00	0.03
BGM@4	3.922	0.036	2.535	0.223	89	18	-16	126	98	0.56	0.07
BGM@5	4.377	0.088	3.001	0.292	104	25	-20	69	48	0.61	0.08
BGM@6	3.003	0.071	2.361	0.065	130	13	-12	713	721	0.70	0.03
BGM@7	4.627	0.109	0.887	0.086	4.9	2.5	-2.4	314	206	0.04	0.02
BGM@8	2.583	0.096	2.427	0.164	232	172	-64	135	159	0.88	0.09
BGM@9	3.701	0.084	2.828	0.188	128	25	-21	149	122	0.69	0.06
BGM@10	3.724	0.137	0.863	0.076	5.5	2.9	-2.8	296	241	0.05	0.02
BGM@11	3.608	0.085	3.308	0.251	226	130	-58	122	102	0.87	0.09
BGM@12	3.842	0.088	3.139	0.028	154	38	-28	142	113	0.76	0.07
BGM@13	3.989	0.108	3.178	0.267	145	41	-30	132	100	0.74	0.08
BGM@14	4.237	0.098	2.859	0.294	99	25	-20	170	122	0.60	0.08
BGM@15	3.215	0.075	2.677	0.119	157	26	-21	222	210	0.76	0.05
BGM@16	2.889	0.072	2.201	0.116	118	20	-17	303	318	0.66	0.06
Whole rock	0.628	0.007	0.705	0.007							

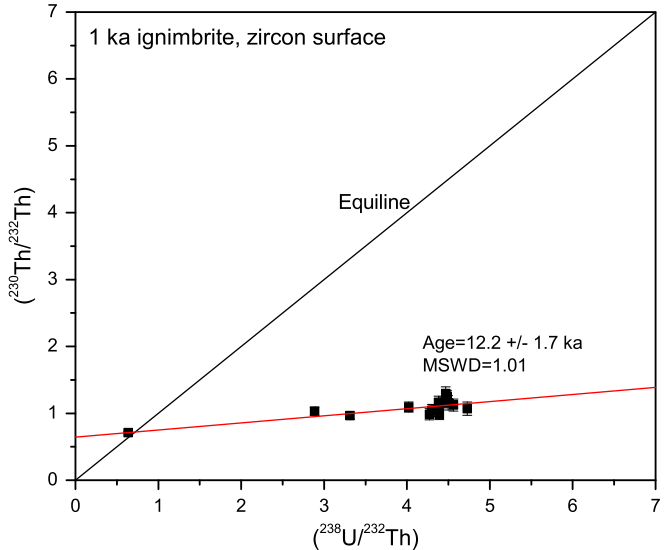
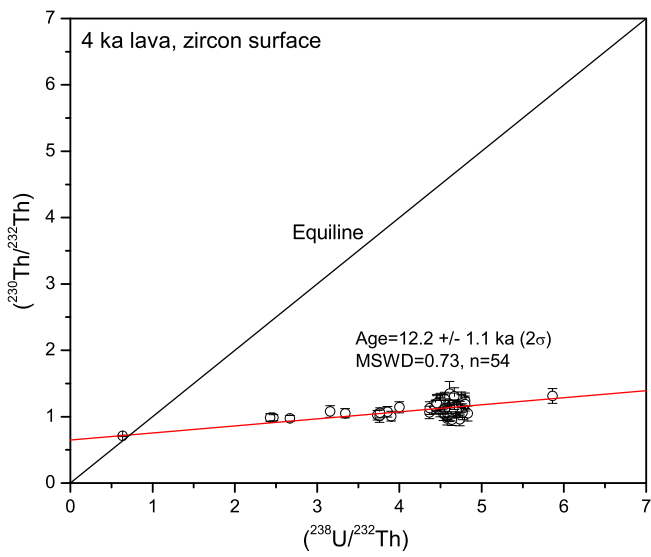


Fig. 4. Zircon equilibration plot for the 4-ka comenditic lava at Qixiangzhan. Whole-rock U-Th isotope data sources: Zou et al. (2008). ISOPLOT 3.00 is used in the calculation (Ludwig, 2003).

Fig. 5. Zircon equilibration plot for the 1-ka comenditic ignimbrite near Baiyanfeng (BYFX).

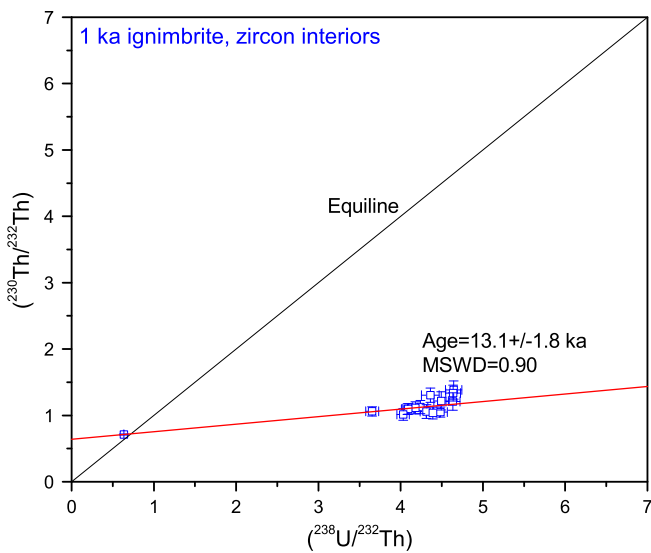


Fig. 6. Zircon interior equiline plot for the 1-ka ignimbrite BYFX.

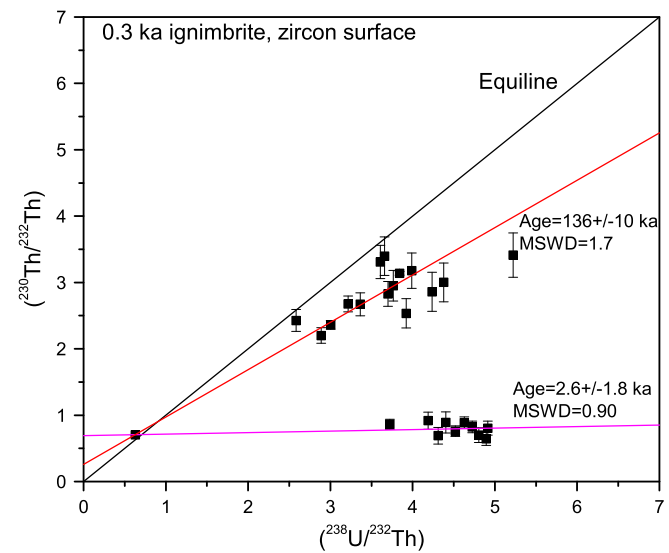


Fig. 8. Zircon equiline plot for the 0.3-ka trachytic ignimbrite. The three zircons close to the equiline are not used to calculate the 136 ka isochron.

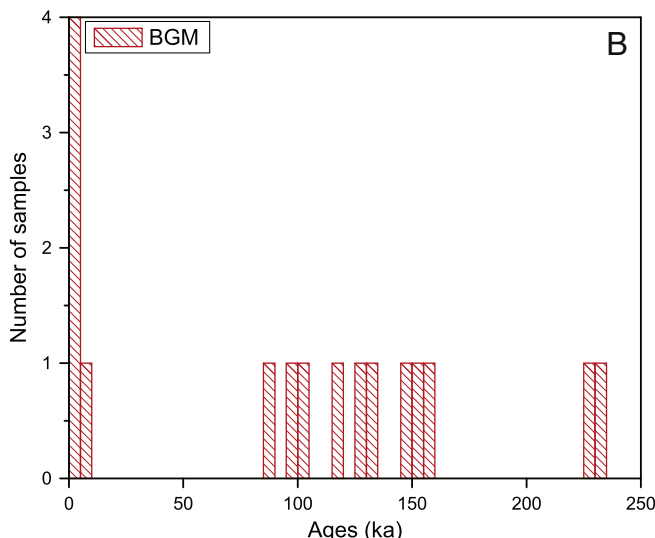
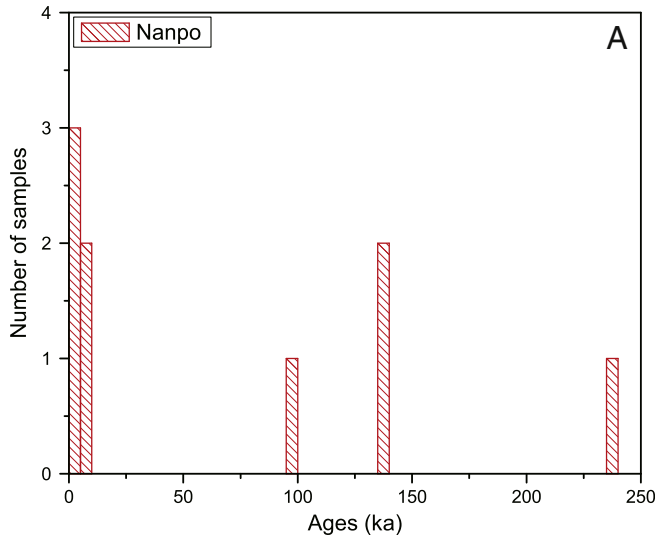


Fig. 7. Zircon model age distributions for the 0.3-ka trachytic ignimbrite from Nanpo and Baguamiao.

QXZ lavas, 0.512571 for 1-ka pumice, and 0.512542 for 1-ka ignimbrite (Fan et al., 1999). Thus the 4-ka QXZ lava provides an early sampling of a much larger magma body at depth and serves as an early-warning petrological signal. Our work also contributes to the growing database of less voluminous lavas preceding massive caldera-forming eruptions, such as the Cleetwood lava preceding the Mt Mazama eruption (Bacon, 1983), the Pagosa Peak dacite preceding the Fish Canyon tuff (Bachmann et al., 2000), and the pre-Ammonia Tanks rhyolite lava preceding the Ammonia Tanks eruption (Bindeman et al., 2006). Compared with available work in the literature, our age data provide higher precision and resolution due to the relative youngness of the Changbai eruptions and associated zircons.

5.2. Change of magma plumbing system after the 1-ka climactic caldera-forming eruption

Zircon age distributions from multiple eruptions of the same volcano can be used to evaluate the evolution of a volcanic plumbing system that may not be detected by present-day geophysical measurements. When plotting the distributions of zircon model ages for all three eruptions (Fig. 9A–D), the 4-ka eruption and 1-ka eruption have the same unimodal distribution. In contrast, the 0.3-ka eruption shows multimodal distributions, and has two much older populations and one younger population than the 4-ka eruption and 1-ka eruption. There is essentially no overlap in model ages between the 0.3-ka eruption and older (4-ka and 1-ka) eruptions. Since the uncertainty in isochron slope (instead of model ages) is symmetrical with respect to the slope value, the distribution of the two-point isochron slopes also can be used to compare zircon age populations. The distribution of isochron slopes for Changbai also suggests a clear distinction between the 0.3-ka eruption and earlier comendites (Fig. 9E–H). In addition, as mentioned earlier, the minerals in the 0.3-ka post-caldera trachytic ignimbrites are more enriched in Ca and Mg. For example, the sanidine An number is 4.8 for the 0.3-ka trachytic ignimbrites but less than 1.0 for the 4-ka comendite lava and the 1-ka comenditic ignimbrite and pumice; the En number in clinopyroxene is 13.2 for the 0.3-ka trachytic ignimbrites but less than 4.1 for the 4-ka comendite lava and the 1-ka comenditic ignimbrite and pumice (Fan et al., 1999). Furthermore, SiO₂ content (64–66 wt%) in the post-caldera ignimbrite differs from the pre-caldera and syn-caldera eruptions (72–74 wt% SiO₂) (Table 1). Thus, based on

Table 3

Chemical compositions of feldspar and glass from 1-ka ignimbrite measured by electron microprobe.

	Feldspar	Glass	Glass	Glass	Glass												
SiO ₂	67.53	67.64	66.87	67.24	65.98	67.00	66.99	66.98	66.75	64.98	67.05	66.94	66.69	75.50	77.34	75.26	74.30
TiO ₂	0.02	0.00	0.05	0.00	0.00	0.03	0.00	0.02	0.06	0.04	0.00	0.07	0.03	0.20	0.24	0.18	0.20
Al ₂ O ₃	18.49	18.61	18.44	18.99	18.23	18.39	18.43	18.49	18.29	18.09	18.54	18.35	18.54	9.96	10.38	10.12	10.04
FeO	0.31	0.28	0.30	0.23	0.25	0.28	0.33	0.25	0.26	0.26	0.32	0.23	0.23	4.09	4.01	4.02	3.91
MnO	0.03	0.03	0.00	0.00	0.00	0.00	0.00	0.00	0.02	0.00	0.00	0.00	0.00	0.05	0.06	0.08	0.05
MgO	0.03	0.00	0.00	0.00	0.00	0.00	0.02	0.01	0.02	0.02	0.00	0.00	0.01	0.00	0.04	0.04	0.03
CaO	0.06	0.12	0.16	0.25	0.21	0.17	0.08	0.17	0.22	0.28	0.07	0.14	0.26	0.23	0.18	0.15	0.17
Na ₂ O	7.66	7.92	8.00	7.91	6.75	7.38	7.23	7.18	7.20	6.86	7.13	7.02	7.54	5.55	5.61	5.52	5.50
K ₂ O	6.48	5.63	5.60	5.89	6.61	6.61	6.57	6.53	6.64	6.17	6.52	6.50	6.18	4.46	4.40	4.31	4.45
Cr ₂ O ₃	0.00	0.02	0.03	0.02	0.11	0.00	0.04	0.00	0.00	0.38	0.03	0.00	0.00	0.01	0.03	0.00	0.02
NiO	0.02	0.04	0.07	0.00	0.01	0.00	0.05	0.00	0.00	0.02	0.00	0.00	0.00	0.00	0.00	0.00	0.00
Total	101	100	99.5	101	98.2	99.9	99.7	99.6	99.4	97.1	99.7	99.2	99.5	100	102	99.7	98.7
Wo %																	
En %																	
Fs %																	
Fo %																	

Pressure is assumed to be 0.3 GPa (about 10 km). The temperature estimate is insensitive to pressure change.

For example, increasing pressure from 0.3 GPa to 0.4 GPa only increases temperature estimate by 0.1 °C.

cpx = clinopyroxene.

^a Average glass composition, along with individual alkali feldspar, is used for the calculation of magma composition.^b Temperature is calculated from alkali feldspar-glass pairs using Equation 24b for volcanic systems from Putirka (2008).

zircon U-series ages, as well as mineral and whole-rock chemistry, Changbai's magmatic plumbing system remained the same between the 4-ka eruption and the 1-ka Millennium Eruption, but changed after the caldera-forming Millennium Eruption.

The distinctive zircon age spectrum in the post-caldera 0.3-ka eruption suggests that post-caldera eruptions are derived from an independent magma reservoir that captured older pre-existing zircon crystals. In contrast, the pre-caldera and syn-caldera eruptions did not capture these older crystals. Note that changes in the subvolcanic reservoir induced by the caldera collapse have been observed in Long Valley, California (Hildreth, 2004), based on changes in the type and style of volcanism following the 760-ka caldera-forming eruptions. The Long Valley 760-ka climactic eruption is beyond the practical age limit for U-series zircon dating (350 ka). Both the 1-ka caldera-forming eruption and the 0.3-ka post-caldera eruption of the Changbai volcano provide an exceptional opportunity to use the unique and powerful U-series zircon dating to evaluate possible changes in the magma plumbing system after the climactic caldera-forming eruptions.

5.3. Zircon residence times, growth rate, and magma residence times

Zircon ages can be used to constrain crystal residence times when coupled with eruption ages. Since zircon isochron ages from the 4 ka and 1 ka eruptions are 12 ka, the zircon residence times are 8 thousand years (8 kyr) for the 4-ka eruption and 11 kyr for the 1 ka eruption. Apparent zircon pre-eruption times of 8 to 11 kyr are rather short for rhyolitic magmas.

The zircon rim and interior age data for the 1-ka ignimbrite can be used to assess zircon growth rates. The nearly identical interior (13.1 ± 1.8 ka) and rim (12.2 ± 1.7 ka) isochron ages within 0.9 ± 2.5 ka suggest rapid zircon crystallization. The maximum possible growth period for the zircons is 3.4 kyr ($=0.9 + 2.5$ ka). Using a typical grain size of 50 µm (as observed for the Changbai zircons), the minimum zircon growth rate is 2.3×10^{-14} cm/s, at the high end of the theoretical range for zircon growth rate (10^{-17} – 10^{-13} cm/s) (Watson, 1996). A more rigorous estimate of zircon growth rate can be obtained by deep depth profiling (Grove and Harrison, 1999; Schmitt, 2011; Storm et al., 2012). But this deep depth profiling method is more time consuming

and expensive, and is not definitively needed for the Changbai zircons, where zircon interior and rim have almost identical ages.

Note that the depth of surface profiling (3 µm) for zircons from the Changbai 1-ka ignimbrite only represents growth in less than 0.2 kyr, which is significantly smaller than the zircon pre-eruption residence time (11 ka) for the 1-ka eruption. Thus, the 11-kyr hiatus between the final zircon growth (measured by surface profiling) and eruption age for the 1-ka eruption is not an analytical artifact, because 3-µm surface profiling only represents 0.2 kyr zircon growth in this case.

Zircon pre-eruption residence times for most rhyolitic magmas range from 25 kyr to several hundred thousands years (Bachmann et al., 2007; Bacon and Lowenstern, 2005; Brown and Fletcher, 1999; Halliday et al., 1989; Mahood, 1990; Reagan et al., 2003; Simon et al., 2008). Since zircon saturation temperature is usually high in silicic magmas, zircon residence time may represent magma residence time. However, interpretation of zircon pre-eruption ages in terms of magma residence times can be complex (Charlier and Wilson, 2010; Klemetti et al., 2011; Wilson and Charlier, 2009) and zircon pre-eruption crystallization ages may not always represent magma residence times. The interpretation of magma residence time is more complex for those protracted zircon age spans (several hundred thousands years). Some protracted zircon crystallization may reflect remobilization of earlier intrusions or crystal mush (Mahood, 1990), rather than long standing magma chambers. Nevertheless, for zircons with a short age span and simple age spectra, such as the case for the zircons from the 4-ka and 1-ka eruptions, the interpretation of zircon residence time as magma residence time can be less problematic. We suggest that the magma residence times are 8 kyr for the 4-ka eruption and 11–12 kyr for the 1-ka eruption. Even if the zircons from the 4-ka eruption and 1-ka eruption are antecrysts from earlier magmatic events, zircon residence times still provide the maximum magma residence times. The very young zircon ages from Changbai nevertheless provide a tight and robust maximum age constraint for magma residence times.

The zircons from the 0.3-ka eruption display multi-modal age distributions with 3 peaks. Bimodal or multi-modal zircon age distributions may indicate the presence of antecrystal or xenocrystal zircons (Charlier et al., 2005). The youngest mode (2.6 ± 1.8 ka) from the 0.3

Glass	Ave glass ^a	cpx	ol	ol	ol	ol	Average									
74.21	75.32	49.06	49.78	49.52	49.73	49.37	49.33	48.88	49.22	49.48	49.31	30.16	30.23	30.23	30.43	
0.17	0.20	0.31	0.19	0.16	0.19	0.28	0.34	0.42	0.23	0.27	0.26	0.06	0.00	0.05	0.00	
9.91	10.08	0.16	0.16	0.14	0.13	0.12	0.30	0.10	0.14	0.14	0.01	0.01	0.01	0.01	0.01	
3.99	4.01	27.98	28.73	28.52	28.14	28.58	27.77	27.85	28.60	28.50	28.72	66.27	67.11	67.05	66.98	
0.09	0.07	0.79	0.89	0.78	0.72	0.78	0.96	0.98	0.80	0.82	0.79	2.28	2.43	2.42	2.33	
0.01	0.02	1.22	1.37	1.38	1.45	1.06	1.36	1.48	1.04	1.06	0.98	0.83	0.75	0.77	0.83	
0.17	0.18	17.57	17.61	17.77	17.63	17.74	19.24	19.27	17.85	17.69	17.75	0.21	0.19	0.18	0.18	
5.31	5.50	1.80	1.77	1.69	1.72	1.88	0.73	0.68	1.80	1.61	1.80	0.03	0.00	0.04	0.06	
4.30	4.38	0.02	0.00	0.00	0.00	0.04	0.00	0.02	0.03	0.02	0.03	0.00	0.00	0.00	0.02	
0.02	0.02	0.01	0.02	0.00	0.00	0.02	0.00	0.02	0.01	0.02	0.00	0.06	0.03	0.00	0.02	
0.00	0.00	0.00	0.00	0.01	0.00	0.00	0.02	0.00	0.01	0.00	0.00	0.06	0.09	0.05	0.02	
98.2	99.8															0.358
																0.634
																0.008
																732
45.26	44.57	44.90	44.35	45.78	44.95	45.19	45.88	44.41	45.53							45.08
4.37	4.83	4.86	5.06	3.80	4.42	4.83	3.73	3.71	3.51							4.31
50.37	50.60	50.24	50.60	50.42	50.63	49.98	50.39	51.88	50.96							50.61
																2.10
																1.88
																1.93
																2.08
																2.00

eruption represents zircon microphenocrysts (autocrysts) that crystallized in a trachytic magma chamber in the buildup to the 0.3-ka eruption. The 130 ka and >230 ka zircons may represent antecrysts derived from earlier episodes of magmatism, or those zircons formed at depth if the magma body stalled at multiple depths. If this interpretation is correct, the zircon storage time in the final eruptible magma body for the 0.3 ka eruption is 2.3 ± 1.8 ka. Compared with literature data (Dosseto and Turner, 2011; Simon et al., 2008), the magma residence time for the 0.3-ka trachytic eruption is exceptionally short.

5.4. Magma temperature

The lack of co-existing Fe–Ti oxides, coexisting feldspars, or coexisting pyroxenes in the recent Changbai eruption products prevents the application of these conventional geothermometers to estimate magma temperature. These recent eruption products contain alkali feldspar, clinopyroxene, and glass. Since the Changbai clinopyroxene is iron-rich hedenbergite (1–1.5 wt.% MgO, 27.8–28.7 wt.% FeO) (e.g., Table 3) and hedenbergite was not used in the calibration of clinopyroxene–glass geothermometry, the clinopyroxene–glass geothermometry method may not be suitable for the Changbai hedenbergite.

As a result, we use an alkali feldspar–glass geothermometer for volcanic rocks (Putirka, 2008) to estimate magma temperature. Based on the chemical compositions of alkali feldspar and glass for the 4-ka lava and 0.3-ka ignimbrite from Fan et al. (1999), the magma temperature is 710 °C for the 4-ka lava and 740 °C for the 0.3-ka ignimbrite. Based on our new chemical data for the 1-ka ignimbrite in Table 3, average magma temperature for the 1-ka ignimbrite is 732 °C. The temperature range (710–740 °C) estimated from the alkali feldspar–glass geothermometer for the recent eruptions in the Changbai volcano is similar to the lower end of the temperature range (720–790 °C) for the rhyolitic Bishop Tuff (California) estimated by an Fe–Ti oxide geothermometer (Hildreth, 1979). At present the extent of possible systematic errors between Fe–Ti oxide temperature and the alkali feldspar–glass temperature is unclear.

Magma temperature (710 °C) of the 4-ka lava is slightly lower than that (732 °C) of the 1-ka ignimbrite. Since zircon-age data suggest that the 4-ka and 1-ka eruptions shared the same magma chamber, there might be a moderate temperature gradient in this magma

chamber. If this temperature difference (22 °C) calculated from the same geothermometer is real, then the cooler magma erupted at 4 ka and the main magma erupted at 1 ka form a thermally zoned magma chamber. This eruption sequence is consistent with the suggestion that the lowest-temperature magma in the roof zone of a thermally zoned magma chamber usually escapes first (Hildreth, 1981).

6. Conclusions

- (1) U-series isochron ages are 12.2 ± 1.1 ka (2σ) for zircon rims from the 4-ka comendite lavas, 12.2 ± 1.7 ka for zircon rims from the 1-ka comenditic ignimbrite, and 13.1 ± 1.8 ka for zircon interiors from the same 1-ka ignimbrite. The 0.3-ka trachytic ignimbrites show multi-modal distributions of zircon rim ages at 2.6 ± 1.8 ka, 136 ± 10 ka, and >230 ka.
- (2) The indistinguishable zircon ages for the pre-caldera 4-ka eruption of comendite lava and syn-caldera 1-ka eruption of comendite pumice and ignimbrite suggest that the 4-ka lava provides an early sampling of a much larger magma body at depth and serves as an early-warning petrological signal. The 4-ka eruption tapped the low-temperature (710 °C) magma near the roof of a thermally zoned magma chamber that generally escaped first.
- (3) The distinct multi-modal zircon age distributions for the 0.3-ka eruption of trachytic magma reveal that this post-caldera eruption tapped a separate magma chamber, and argue against any significant mixing between comendite and the 0.3-ka trachyte magma bodies at Changbai. The comendites and the 0.3-ka trachytes themselves represent distinct magma batches. Changbai's magmatic plumbing system changed after the 1-ka climactic caldera-forming Millennium Eruption.
- (4) Zircon residence times for the moderate 4-ka, large 1-ka and small 0.3-ka eruptions at Changbai are 8 kyr, 11–12 kyr and 2.3 kyr, respectively, and are negatively correlated with their eruption volumes. These overall short magma residence times for all 3 eruptions likely suggest that the Changbai volcano is potentially a highly dangerous volcano once a magma body is formed. The extremely short magma residence time for the 0.3-ka trachytic eruption might suggest higher probability and frequency for a small-scale trachytic eruption in the future.

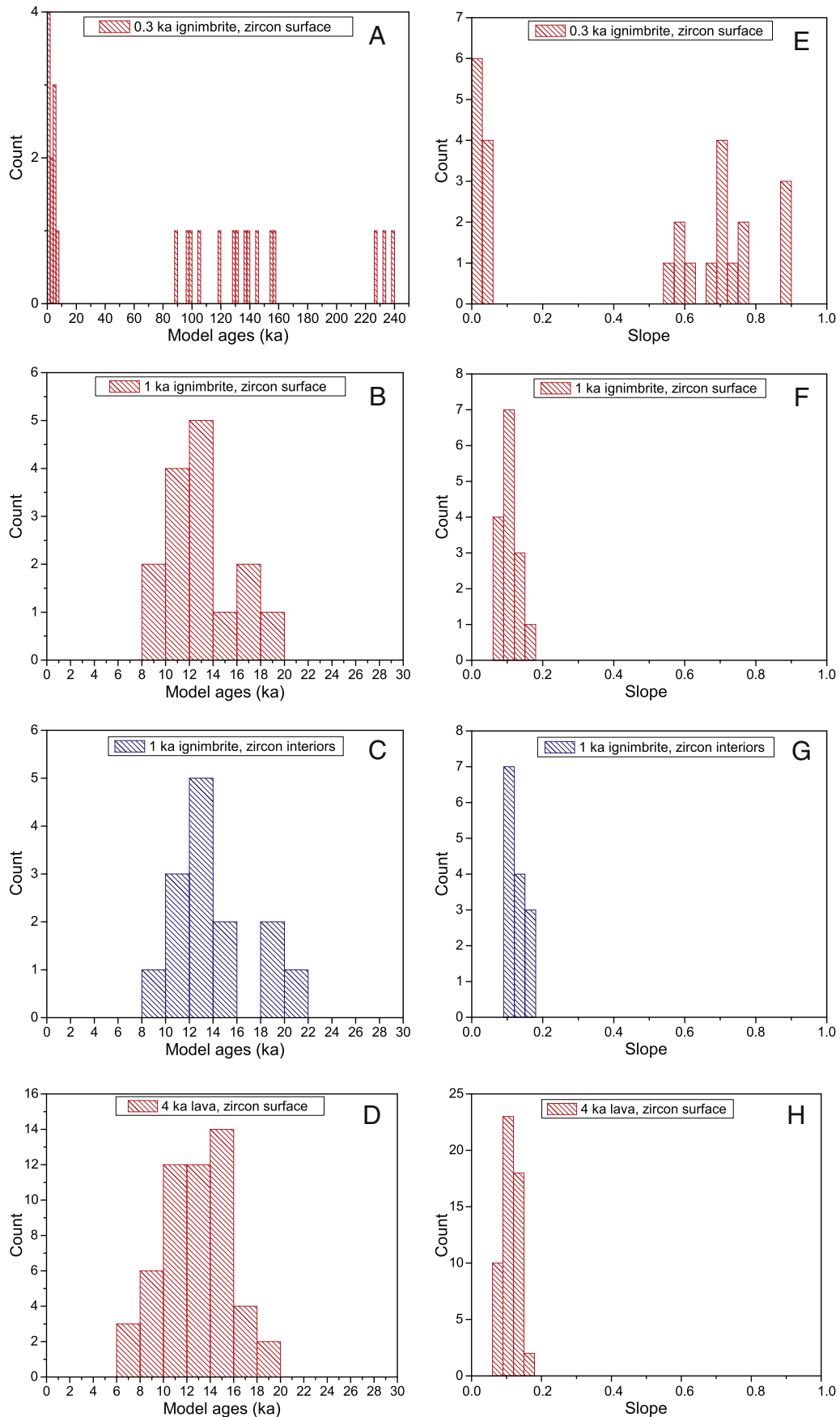


Fig. 9. (A-D, left panel) Comparison of model age distributions between the 4-ka, 1-ka and 0.3-ka eruptions. Note that the scale in model ages for the 0.3-ka eruption is different from the 4-ka and 1-ka eruptions, but the bin size (2 ka) is kept the same for clear comparison; (E-H, right panel) comparison of two-point isochron slope distributions between the 4-ka, 1-ka, and 0.3-ka eruptions. One advantage of the slope diagram is that the maximum limit in the x-axis is 1.0 and thus it is easy to keep the same x-axis scale. Bin size = 0.03.

Acknowledgments

This work is supported by a US NSF grant EAR-1119077 (to Zou). The ion probe facility at UCLA is in part supported by a grant from the NSF Earth Sciences Instrumentation and Facility program. Jennifer Garrison, an anonymous reviewer, and journal editor Andrew Kerr provided very constructive reviews that have significantly improved the quality of this paper. We are also grateful to Qian Mao for his assistance with electron probe analyses and to Erin Summerlin (Auburn University) for polishing this paper.

References

- Bachmann, O., Dungan, M.A., Lipman, P.W., 2000. Voluminous lava-like precursor to a major ash-flow tuff: low-column pyroclastic eruption of the Pagosa Peak Dacite, San Juan volcanic field, Colorado. *Journal of Volcanology and Geothermal Research* 98, 153–171.
- Bachmann, O., Charlier, B.L.A., Lowenstern, J.B., 2007. Zircon crystallization and recycling in the magma chamber of the rhyolitic Kos Plateau Tuff (Aegean arc). *Geology* 35, 73–76.
- Bacon, C.R., 1983. Eruptive history of Mount Mazama and Crater Lake caldera, Cascade Range, U.S.A. *Journal of Volcanology and Geothermal Research* 18, 57–115.
- Bacon, C.R., Lowenstern, J.B., 2005. Late Pleistocene granodiorite source for recycled zircon and phenocrysts in rhyodacite lava at Crater Lake, Oregon. *Earth and Planetary Science Letters* 233, 277–293.
- Basu, A.R., Wang, J.W., Huang, W.K., Xie, G.H., Tatsumoto, M., 1991. Major element, REE, and Pb, Nd and Sr isotopic geochemistry of Cenozoic volcanic rocks of eastern China: implications for their origin from suboceanic-type mantle reservoirs. *Earth and Planetary Science Letters* 105, 149–169.
- Bindeman, I.N., Schmitt, A.K., Valley, J.W., 2006. U-Pb zircon geochronology of silicic tuffs from the Timber Mountain/Oasis Valley caldera complex, Nevada: rapid generation of large volume magmas by shallow-level remelting. *Contributions to Mineralogy and Petrology* 152, 649–665.
- Brown, S.J.A., Fletcher, I.R., 1999. SHRIMP U-Pb dating of the preeruption growth history of zircons from the 340 ka Whakamaru Igneous Suite, New Zealand: evidence for >250 k.y. magma residence times. *Geology* 27, 1035–1038.
- Charlier, B.L.A., Wilson, C.J.N., 2010. Chronology and evolution of caldera-forming and post-caldera magma systems at Okataina volcano, New Zealand from zircon U-Th model-age spectra. *Journal of Petrology* 51. <http://dx.doi.org/10.1093/petrology/eqq1015>.
- Charlier, B.L.A., Wilson, C.J.N., Lowenstern, J.B., Blake, S., Van Calsteren, P.W., Davidson, J.P., 2005. Magma generation at a large, hyperactive silicic volcano (Taupo, New Zealand) revealed by U-Th and U-Pb systematics in zircons. *Journal of Petrology* 46, 3–32.
- Condoni, M., 1997. Dating recent volcanic rocks through ^{230}Th – ^{238}U disequilibrium in accessory minerals: example of the Puy de Dome (French Massif Central). *Geology* 25, 375–378.
- Dosseto, A., Turner, S.P., 2011. Magma cooling and differentiation – uranium-series isotopes. In: Dosseto, A., Turner, S.P., Van Orman, J.A. (Eds.), *Timescales of Magmatic Processes: From Core to Atmosphere*. Wiley-Blackwell, pp. 160–180.
- Dunlap, C.E., Gill, J.B., Palacz, Z.A., 1992. U/Th disequilibria in the large-volume chemically-zoned eruption of Baitoushan, 1010 AD. *Eos, Transactions American Geophysical Union* 73, 611.
- Fan, Q.C., Liu, R.X., Wei, H.Q., Sui, J.L., Li, N., 1999. The characteristics of petrogeochemistry of Holocene eruption at Changbaishan Tianchi volcano. *Geological Review* 45, 263–271.
- Fan, Q.C., Sui, J.L., Wang, T.H., Li, L., Sun, Q., 2006. Eruption history and magma evolution of the trachybasalt in the Tianchi volcano, Changbaishan. *Acta Petrologica Sinica* 22, 1449–1457.
- Grove, M., Harrison, T.M., 1999. Monazite Th–Pb age depth profiling. *Geology* 27, 487–490.
- Halliday, A.N., Mahood, G.A., Holden, P., Metz, J.M., Dempster, T.J., Davidson, J.P., 1989. Evidence for long residence times of rhyolitic magma in the Long Valley magmatic system: the isotopic record in precaldera lavas of Glass Mountain. *Earth and Planetary Science Letters* 94, 274–290.
- Hildreth, W., 1979. The Bishop Tuff: evidence for the origin of compositional zonation in silicic magma chambers. *Geological Society of America, Special Paper* 180, 43–75.
- Hildreth, W., 1981. Gradients in silicic magma chambers: implications for lithospheric magmatism. *Journal of Geophysical Research* 86, 10153–10192.
- Hildreth, W., 2004. Volcanological perspectives on Long Valley, Mammoth Mountain, and Mono Craters: several contiguous but discrete systems. *Journal of Volcanology and Geothermal Research* 136, 169–198.
- Horn, S., Schmincke, H.U., 2000. Volatile emission during the eruption of Baitoushan Volcano (China/North Korea) ca. 969 AD. *Bulletin of Volcanology* 61, 537–555.
- Ji, F.J., Li, J.P., Zheng, R.Z., 1999. The preliminary study of TL chronology for recent eruptive materials in Changbaishan Tianchi volcano, Changbai Mountains. *Geological Review* 45, 287–293.
- Johnson, D.M., Hooper, P.R., Conrey, R.M., 1999. XRF analysis of rocks and minerals for major and trace elements on a single low dilution Li-tetraborate fused bead. *JCPDS – International Centre for Diffraction Data* pp. 843–867.
- Klemetti, E.W., Deering, C.D., Cooper, K.M., Roeske, S.M., 2011. Magmatic perturbations in the Okataina Volcanic Complex, New Zealand at thousand-year timescales recorded in single zircon crystals. *Earth and Planetary Science Letters* 305, 185–194.
- Kuritani, T., Kimura, J.K., Miyamoto, T., Wei, H.Q., Shimano, T., Maeno, F., Jin, X., Taniguchi, H., 2009. Intraplate magmatism related to deceleration of upwelling asthenospheric mantle: implications from the Changbaishan shield basalts, northeast China. *Lithos* 112, 247–258.
- Li, N., Fan, Q.C., Sun, Q., Zhang, W.L., 2004. Magma evolution of Changbaishan Tianchi volcano: evidence from the main phenocrystal minerals. *Acta Petrologica Sinica* 20, 575–582.
- Liu, R.X., Wei, H.Q., Li, J.T., 1998. The Latest Eruptions From the Tianchi Volcano, Changbaishan. *SciencePress, Beijing*.
- Liu, J.Q., Han, J.T., Fyfe, W.S., 2001. Cenozoic episodic volcanism and continental rifting in northeast China and possible line to Japan Sea development as revealed from K-Ar geochronology. *Tectonophysics* 339, 385–401.
- Liu, Y.S., Nie, B.F., Sun, S.P., Mo, D.W., Shi, Y.S., 2007. Petrology of comenditic lava from the eruption at Late Qixiangzhan stage in Tianchi volcano, Changbaishan area. *Geoscience* 21, 296–306.
- Lowenstern, J.B., Persing, H.M., Wooden, J.L., Lanphere, M., Donnelly-Nolan, J., Grove, T.L., 2000. U-Th dating of single zircons from young granitoid xenoliths: new tools for understanding volcanic processes. *Earth and Planetary Science Letters* 183, 291–302.
- Ludwig, K.R., 2003. User's Manual for ISOPLOT 3.00: A Geochronological Toolkit for Microsoft Excel, Berkeley.
- Machida, H., Arai, F., 1983. Extensive ash falls in and around the Sea of Japan from large late Quaternary eruptions. *Journal of Volcanology and Geothermal Research* 18, 151–164.
- Mahood, G.A., 1990. Second reply to comment of R. S. J. Sparks, H. E. Huppert and C. J. N. Wilson on "Evidence for long residence times of rhyolitic magma in the Long Valley magmatic system: the isotopic record in the precaldera lavas of Glass Mountain". *Earth and Planetary Science Letters* 99, 395–399.
- Nakamura, T., Okuno, M., Kimura, K., Mitsutani, T., Moriaki, H., Ishizuka, Y., Kim, K.H., 2007. Application of ^{14}C wiggle-matching to support dendrochronological analysis in Japan. *Tree-Ring Research* 63, 37–46.
- Paces, J.B., Miller, J.D., 1993. Precise U-Pb ages of Duluth complex and related mafic intrusions, northeastern Minnesota – geochronological insights to physical, petrogenetic, paleomagnetic, and tectonomagmatic processes associated with the 1.1 Ga midcontinent rift system. *Journal of Geophysical Research* 98, 13997–14013.
- Putirka, K.D., 2008. Thermometers and barometers for volcanic systems. In: Putirka, K.D., Tepley III, F.J. (Eds.), *Minerals, Inclusions and Volcanic Processes: Reviews in Mineralogy and Geochemistry*. Mineralogical Society of America, Chantilly, VA, pp. 61–120.
- Reagan, M.K., Sims, K.W.W., Erich, J., Thomas, R.B., Cheng, H., Edwards, R.L., Layne, L., Ball, L., 2003. Time-scales of differentiation from mafic parents to rhyolite in North American continental arcs. *Journal of Petrology* 44, 1703–1726.
- Reid, M.R., Coath, C.D., Harrison, T.M., McKeegan, K.D., 1997. Prolonged residence times for the youngest rhyolites associated with Long Valley caldera: ion microprobe dating of young zircons. *Earth and Planetary Science Letters* 150, 27–38.
- Schmitt, A.K., 2011. Uranium series accessory crystal dating of magmatic processes. *Annual Review of Earth and Planetary Sciences* 39, 321–349.
- Schmitt, A.K., Wetzel, F., Cooper, K.M., Zou, H.B., Worner, G., 2010. Magmatic longevity of Laacher See Volcano (Eifel, Germany) indicated by U-Th dating of intrusive carbonatites. *Journal of Petrology* 51, 1053–1085.
- Self, S., Rampino, M.R., Newton, M.S., Wolff, J.A., 1984. Volcanological study of the great Tambora eruption of 1815. *Geology* 12, 659–663.
- Simon, J.I., Renne, P.R., Mundil, R., 2008. Implications of pre-eruptive magmatic histories of zircons for U-Pb geochronology of silicic extrusions. *Earth and Planetary Science Letters* 266, 182–194.
- Stone, R., 2011. Vigil at North Korea's Mount Doom. *Science* 334, 5.
- Stone, R., 2013. Sizing up a slumbering giant. *Science* 341, 1060–1061.
- Storm, S., Shane, P., Schmitt, A.K., Lindsay, J.M., 2011. Contrasting punctuated zircon growth in two syn-erupted rhyolite magmas from Tarawera volcano: insight to crystal diversity in magmatic systems. *Earth and Planetary Science Letters* 301, 511–520.
- Storm, S., Shane, P., Schmitt, A.K., 2012. Decoupled crystallization and eruption histories of the rhyolite magmatic system at Tarawera volcano revealed by zircon ages and growth rates. *Contributions to Mineralogy and Petrology* 163, 505–519.
- Su, W., Zhang, M., Redfern, S.A.T., Gao, J., Klemd, R., 2009. OH in zoned amphiboles of eclogite from the Western Tianshan, NW-China. *International Journal of Earth Sciences* 98, 1299–1309.
- Tatsumi, Y., Maruyama, S., Nohda, S., 1990. Mechanism of backarc opening in the Japan Sea: role of asthenospheric injection. *Tectonophysics* 181, 299–306.
- Tucker, R.T., Zou, H.B., Fan, Q.C., Schmitt, A.K., 2013. Ion microprobe dating of zircons from active Dayingshan volcano, Tengchong, SE Tibetan Plateau: time scales and nature of magma chamber storage. *Lithos* 172–173, 214–221.
- Watson, E.B., 1996. Dissolution, growth and survival of zircons during crustal fusion: kinetic principles, geological models and implications for isotopic inheritance. *Transactions of the Royal Society of Edinburgh: Earth Sciences* 87, 43–56.
- Wei, H., Sparks, R.S.J., Liu, R., Fan, Q., Wang, Y., Hong, H., Zhang, H., Chen, H., Jiang, C., Dong, J., Zheng, Y., Pan, Y., 2003. Three active volcanoes in China and their hazards. *Journal of Asian Earth Sciences* 21, 515–526.
- Wei, H.Q., Wang, Y., Jin, J.Y., Gao, L., Yun, S.H., Jin, B.L., 2007. Timescale and evolution of the intracontinental Tianchi volcanic shield and ignimbrite-forming eruption, Changbaishan, Northeast China. *Lithos* 96, 315–324.
- Wei, H.Q., Liu, G.M., Gill, J.B., 2013. Review of eruptive activity at Tianchi volcano, Changbaishan, northeast China: implications for possible future eruptions. *Bulletin of Volcanology* 75, 706.

- Wiedenbeck, M., Alle, P., Corfu, F., Griffin, W.I., Meier, M., Oberli, F., Vonquadt, A., Roddick, J.C., Speigel, W., 1995. 3 natural zircon standards for U-Th-Pb, Lu-Hf, trace-element and REE analyses. *Geostandards Newsletter* 19, 1–23.
- Wilson, C.J.N., Charlier, B.L.A., 2009. Rapid rates of magma generation at contemporaneous magma systems, Taupo volcano, New Zealand: insights from U-Th model-age spectra in zircons. *Journal of Petrology* 50, 34.
- Xu, J.D., Liu, G.M., Wu, J.P., Ming, Y.H., Wang, Q.L., Cui, D.X., Shangguan, Z.G., Pan, B., Lin, X.D., Liu, J.Q., 2012. Recent unrest of Changbaishan volcano, northeast China: a precursor of a future eruption? *Geophysical Research Letters* 39, L16305.
- Yin, G.M., Ye, Y.G., Sun, Y.J., Wan, J.K., Chen, W.J., Diao, S.B., 1999. Electron spin resonance (ESR) dating of recent volcanics from Changbaishan Mountain. *Geological Review* 45, 287–293.
- Zhang, H.F., Sun, M., Zhou, X.H., Fan, W.M., Zhai, M.G., Yin, J.F., 2002. Mesozoic lithosphere destruction beneath the North China Craton: evidence from major-, trace-element and Sr-Nd-Pb isotope studies of Fangcheng basalts. *Contributions to Mineralogy and Petrology* 144, 241–253.
- Zhao, D.P., Tian, Y., Lei, J.S., Liu, L., Zheng, S.H., 2009. Seismic image and origin of the Changbai intraplate volcano in East Asia: role of big mantle wedge above the stagnant Pacific slab. *Physics of the Earth and Planetary Interiors* 173, 197–206.
- Zou, H.B., 2007. Quantitative Geochemistry. Imperial College Press, London.
- Zou, H.B., 2014. Error propagation, In: Holland, H.D., Turekian, K.K. (Eds.), *Treatise on Geochemistry*, Second edition. Elsevier, Oxford, pp. 33–42.
- Zou, H.B., Fan, Q.C., Yao, Y.P., 2008. U-Th systematics of dispersed young volcanoes in NE China: asthenosphere upwelling caused by piling up and upward thickening of stagnant Pacific slab. *Chemical Geology* 255, 134–142.
- Zou, H.B., Fan, Q.C., Schmitt, A.K., Sui, J.L., 2010a. U-Th dating of zircons from Holocene potassie andesites (Maanshan volcano, Tengchong, SE Tibetan Plateau) by depth profiling: time scales and nature of magma storage. *Lithos* 118, 202–210.
- Zou, H.B., Fan, Q.C., Zhang, H.F., 2010b. Rapid development of the great Millennium eruption of Changbaishan (Tianchi) Volcano: evidence from U-Th zircon dating. *Lithos* 119, 289–296.